



DOI: 10.34910/MCE.105.9

Stress condition of brick barrel vaults in view of anisotropic properties

A-Kh.B. Kaldar-ool^{a*}, V.N. Glukhikh^b, E.K. Opbul^b, S.S. Saaya^a

^a Tuva State University, Kyzyl, Republic of Tuva, Russia

^b St. Petersburg State University of Architecture and Civil Engineering, St. Petersburg, Russia

*E-mail: oorzhaka-h@mail.ru

Keywords: barrel vaults, brickwork, elasticity modulus, elasticity constants, elasticity parameters, orthotropic-anisotropic material, cylindrical anisotropy

Abstract. The subject of our studies are brickwork barrel vaults used in historic buildings and structures. To keep flat-arched vaults in good working order, it is required to perform appropriate theoretical research aimed at studying their stress condition. It is necessary to find elastic constants in a new coordinate system in complex curved objects consisting of bricks and mortared joints. To determine elastic constants, we used brickwork strength characteristics obtained from experiments on the basis of known formulas, studied the elastic modulus of bricks and mortar, found the elastic modulus of brickwork with the help of rheology method and used the elasticity parameters interconnecting elastic constants of cylindrical anisotropic bodies in the principal anisotropy directions in new coordinate systems. When assessing the load-bearing capacity of flat-arched vaults, it is possible to determine primary stress values using elastic constants in new coordinate systems with the help of the finite elements method using computer software.

1. Introduction

A brickwork barrel vault [1] is considered as an orthotropic anisotropic body with a cylindrical anisotropy [2] to whom the laws of mechanics of anisotropic bodies may be applied.

The studies [3–12] are the best known ones as regards the methods of analyzing arches and vaults of various shapes. Works [13–25] are experimental studies exploring the strength of brickwork vault structures.

At present, physical and mechanical properties of brickwork are determined in compliance with the requirements of State standards and regulations, in particular, Russian Set of Rules SP 15.13330.2012 [26]. They are examined as those of an elastoplastic material.

Being an anisotropic material, brickwork has different compression, tensile, bending and shear strength values depending on the load direction. In this regard, studies of brickwork barrel vaults with the goal of determining their stress conditions in view of anisotropic properties that allow to assess the carrying capacity of a structure are highly topical.

To reach the set goal, we shall use a numerical method based on the Abaqus 6.14 software package [27]. Whereupon elastic constants of the brickwork entered into the initial data field for calculation were determined using an analytical approach with regard for elasticity parameters in a new system of coordinates.

We have set ourselves the following goal:

1. Experimental determination of the brick and mortar types.
2. Known methods of determining the elasticity modulus of the bricks and the mortar.

Kaldar-ool, A-Kh.B., Glukhikh, V.N., Opbul, E.K., Saaya, S.S. Stress Condition of Brick barrel Vaults in View of Anisotropic Properties. Magazine of Civil Engineering. 2021. 105(5). Article No. 10509. DOI: 10.34910/MCE.105.9

© Kaldar-ool, A-Kh.B., Glukhikh, V.N., Opbul, E.K., Saaya, S.S., 2021. Published by Peter the Great St.Petersburg Polytechnic University



This work is licensed under a CC BY-NC 4.0

3. Brickwork elasticity modulus and anisotropic index depending of the principal anisotropy direction.
4. Determining the brickwork elasticity constants depending on the elasticity parameters needed to carry out a numerical calculation.
5. Numerical calculation.

The following are theoretical studies of a brick barrel vault in an existing building based on actual geometrical and strength characteristics. The studies have been carried out experimentally.

2. Methods

To implement the proposed numerical calculation method, apart from the brick and mortar types, we need to determine their elasticity moduli. According to V.N. Glukhikh, the directions (tangential, radial) of the elastic moduli of the brickwork in the main axes of anisotropy are established.

The brickwork strength was determined ultrasonically using the UK-14P instrument [1].

1. Brick strength limit (surface base equal to 100 mm):

$$R_1 = 7.5201 + 0.008 v_1 \text{ MPa.} \quad (1)$$

- Brickwork mortar strength limit (base equal to 40 mm):

$$R_2 = 7.3975 - 0.0068 v_2 \text{ MPa.} \quad (2)$$

- Brick elasticity modulus is determined according to [28]:

$$E_0^{brick} = 200 \div 1200 \cdot R_{brick}, \quad (3)$$

where R_{brick} is the brick compression strength limit.

- Mortar elasticity modulus is determined according to [29]:

$$E_0^{mortar} = \frac{t_{mortar}}{\lambda_{mortar}}, \quad (4)$$

where t_{mortar} is the thickness of a mortar joint.

λ_{mortar} is compression compliance of a manually laid horizontal mortar joint under short-term loads determined according to the formula:

$$\lambda_{mortar} = 1.5 \cdot 10^{-3} \cdot R_{mortar}^{-\frac{2}{3}} \cdot t_{mortar},$$

R_{mortar} is the mortar strength limit.

We used a phenomenological rheology method in order to find the brickwork elasticity modulus on the main anisotropy axes for a brickwork being under a complex stress [30].

According to [30], one can obtain a realistic picture of the material's behaviour under load by using more complex schemes including both elastic and viscous elements. If we take an elastic material (brick) and a viscous one (mortar) and join them in parallel in the vault head (see Fig. 1, a) and in series near the vault abutments (see Fig. 1, b), we shall obtain rheological models of a Kelvin body and a Maxwell body, respectively [31].

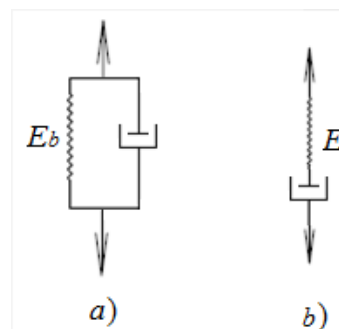


Figure 1. Rheological models.

- a – Kelvin body (the elements are joined in parallel);**
b – Maxwell body (the elements are joined in series).

When the elements are joined in parallel: $M_{brick} = 102$; $R_{1, medium} = 10.03$.

$$E_r = E_0^{brick} + E_0^{mortar} . \quad (6)$$

When the elements are joined in series:

$$E_t = \frac{E_0^{brick} \cdot E_0^{mortar}}{E_0^{brick} + E_0^{mortar}} , \quad (5)$$

Thus, we have obtained elasticity constants E_r , E_t on the main anisotropy directions.

Theoretical studies V.N. Glukhikh have determined that orthotropic cylindrically anisotropic materials differ in elasticity parameters (B_1 , B_2) and can be divided into 2 groups:

- for the first group, the elasticity parameter is characterized by three extremes when axes turn from the radial direction to the tangential one, i.e. from 0° to 90° :

$$B_{(1)} = 3 - k^2 ; \quad (7)$$

- the second group has two extremes:

$$B_{(2)} = \frac{1 + 5k^2}{3} , \quad (8)$$

anisotropic index:

$$k^2 = \frac{E_t}{E_r} . \quad (9)$$

Both parameters are used as multipliers in a fourth-order differential equation in partial derivatives for an orthotropic coordinates; they only depend on relationships between elasticity moduli between the main anisotropy directions.

The graphic illustration of the relationship between elasticity parameters is shown in Fig. 2.

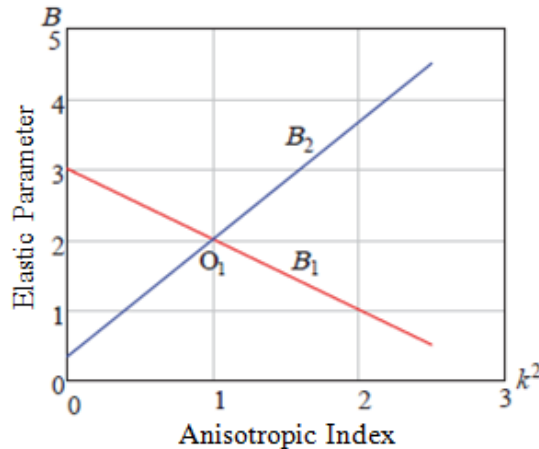


Figure 2. Relationships between an orthotropic body elasticity parameters.

The dependences shown above (see formulas 7 and 8) were deduced mathematically; they interconnect the tension modulus, the shear modulus and the Poisson ratios. This allows to improve the accuracy of determining elasticity constants for anisotropic bodies and to reduce the scope of experimental investigations in accordance with the existing known standards.

In case difficulties arise in determining viscosity constants of, e.g., bricks, mortar joints or brickwork, the result of the calculations may be assessed using the graph shown in Fig. 1 where point O_1 characterizes the isotropic properties of a materials. Both inclined straight lines describe the elasticity properties of anisotropic materials belonging to two groups.

Elasticity constants in a new system of coordinates in view of the first elasticity parameter B_1 (see formulas 7 and 8) of anisotropic bodies will be simplified:

$$\frac{1}{E_x} = \frac{\cos^4 \theta}{E_r} + \frac{\sin^4 \theta}{E_t} + \frac{3 - k^2}{E_t} \cdot \cos^2 \theta \sin^2 \theta ; \quad (10)$$

$$\frac{1}{G_{x'y'}} = \frac{8(k^2 - 1)}{E_t} \cdot \sin^2 \theta \cdot \cos^2 \theta + \frac{1}{G_{rt}}; \tag{11}$$

$$\mu_{x'y'} = -E_{x'} \left[\frac{2(k^2 - 1)}{E_t} \cdot \sin^2 \theta \cdot \cos^2 \theta + \frac{\mu_{rt}}{E_t} \right], \tag{12}$$

where $G_{rt} = \frac{E_t}{3 - k^2 + 2 \cdot \mu_{rt}}$ is the shear modulus.

Elasticity constants in a new system of coordinates in view of the second elasticity parameter B_2 :

$$\frac{1}{E_{x'}} = \frac{\cos^4 \theta}{E_r} + \frac{\sin^4 \theta}{E_t} + \frac{1 + 5k^2}{3E_t} \cdot \sin^2 \theta \cos^2 \theta; \tag{13}$$

$$\frac{1}{G_{x'y'}} = \frac{8 \cdot (1 - k^2)}{3 \cdot E_t} \cdot \sin^2 \theta \cdot \cos^2 \theta + \frac{1}{G_{rt}}; \tag{14}$$

$$\mu_{x'y'} = -E_{x'} \left[\frac{2 \cdot (1 - k^2)}{3 \cdot E_r} \cdot \sin^2 \theta \cdot \cos^2 \theta - \frac{\mu_{rt}}{E_t} \right], \tag{15}$$

where $G_{rt} = \frac{3 \cdot E_t}{1 + 5 \cdot k^2 + 6 \cdot \mu_{rt}}$ is the shear modulus.

Using Abaqus 6.14 software package [27], we have modeled a flat-arched vault having width $b = 1$ m. We have modeled backup in order to take its volume weight into account correctly. The finite element scheme of the vault and the backup is shown in Fig. 3.

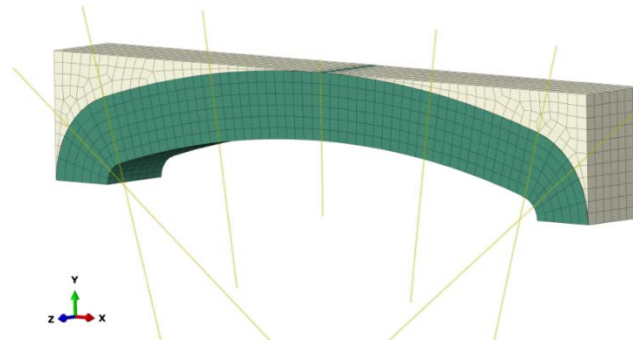


Figure 3. Finite element model.

The vault was modeled as four rigidly connected parts: two parts forming the flat part of the vault and two abutments being small-radius curves. The vault anisotropy scheme was adopted as a cylindrical orthotropic one. The material orientation for the flat and the abutment parts of the vault is shown in Fig. 4.

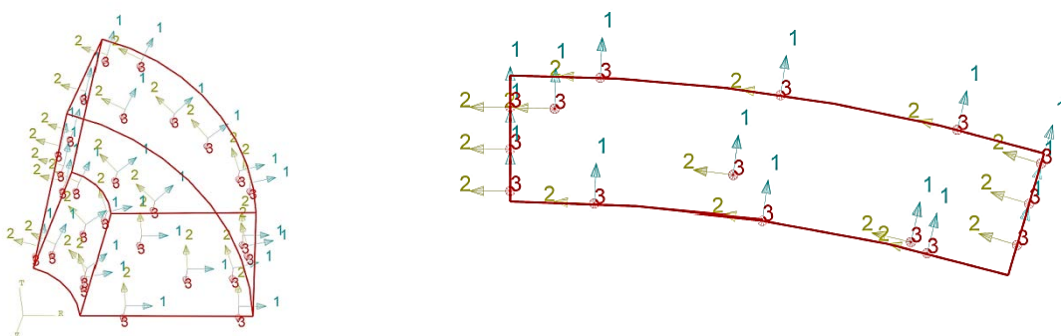


Figure 4. Material orientation for the vault abutment and flat part.

The loads are presented in Fig. 5. Own weight is entered in Abaqus 6.14 by setting gravity on the basis of the brickwork material density. In order to take the reliability coefficient 1.1, the gravity load was increased by this coefficient. The temporary load and the floor load were applied to the horizontal surface

of the backup. Concentrated forces were applied to the backup along the structure central axis at 2 and 3 m distances from the vault head.

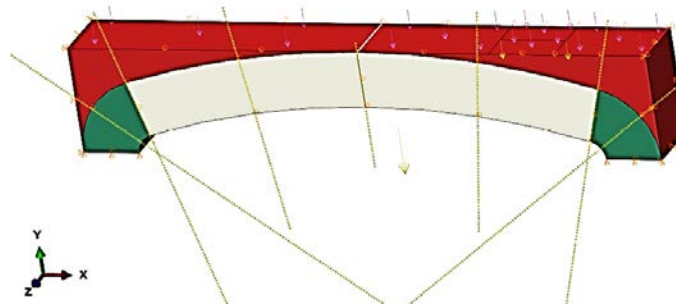


Figure 5. Loads and boundary conditions.

Boundary conditions were set on the basis of the vault design: vertical restraint under the abutments, restraint of the backup end faces along the X axis (see Fig. 5) and restraint of the free sides of the whole structure along the Z axis (in order to take interaction with sister components of the structure into account).

3. Results and Discussion

Table 1. Results of determining brick and mortar strength using the UT nondestructive testing method.

Item No.	t_1 μs	v_1 m/s	R_1 MPa	t_2 μs	v_2 m/s	R_2 MPa	R_i MPa	$p_i = \frac{R_i}{R_{min}}$	$p_i R_i$	$S_i = R_i - R_{med.}$
1	32	3125	10	47	851	1.78	1.14	1.00	1.14	-0.053
2	31	3226	10.1	54	741	2.51	1.25	1.10	1.37	0.056
3	36	2778	9.74	51	784	2.22	1.19	1.04	1.24	-0.006
4	29	3448	10.3	48	833	1.90	1.17	1.03	1.21	-0.019
5	30	3333	10.2	53	755	2.42	1.24	1.09	1.35	0.049
6	34	2941	9.87	49	816	2.01	1.17	1.02	1.19	-0.028

$$R_{med.} = \sum p_i R_i / \sum p_i = 1.19 \text{ MPa.}$$

$$\Delta R = \sqrt{\frac{\sum p_i s_i^2}{(n-1) \sum p_i}} = 0.12 \text{ MPa.}$$

Design brickwork resistance:

$$R = R_{medium} - \Delta R = 1.07 \text{ MPa or } 10.92 \text{ kg/cm}^2;$$

at average value:

$$1. \text{ brick grade } M_{brick} = 102; R_{1, medium} = 10.03 \text{ MPa};$$

$$\text{mortar grade } M_{mortar} = 22; R_{2, medium} = 2.14 \text{ MPa.}$$

Using formulas (3, 4), we obtained the brick and mortar elasticity moduli:

$$E_0^{brick} = 1200 \cdot R_{brick} = 1200 \cdot 10.3 = 12036 \text{ MPa.}$$

$$\begin{aligned} E_0^{mortar} &= \frac{t_{mortar}}{\lambda_{mortar}} = \frac{t_{mortar}}{1.5 \cdot 10^{-3} \cdot R_{mortar}^{-\frac{2}{3}} \cdot t_{mortar}} = \\ &= 1.5 \cdot 10^3 \cdot R_{mortar}^{\frac{2}{3}} = 1.5 \cdot 10^3 \cdot 2.14^{\frac{2}{3}} = 2140 \text{ MPa.} \end{aligned}$$

Theoretical brick and mortar elasticity moduli calculated according to formulas (3, 4), e.g., at $k^2 = 0.5$ are presented in Tables 2–5.

Table 2. Theoretical brick elasticity modulus at $B_{(1)} = 3 - k^2$ ($E_0 = 12036$ MPa).

θ°	0°	15°	30°	45°	60°	75°	90°
$k^2 = 0.5$	24072	20190	14810	12036	11330	11700	12036

Table 3. Theoretical brick elasticity modulus at $B_{(2)} = \frac{1+5k^2}{3}$ ($E_0 = 12036$ MPa).

θ°	0°	15°	30°	45°	60°	75°	90°
$k^2 = 0.5$	24072	23480	21400	18050	14810	12730	12036

Brick elasticity modulus anisotropy is shown in Fig. 6.

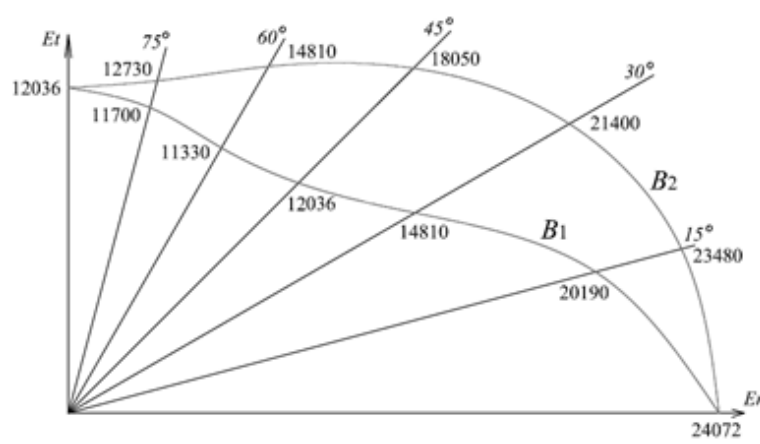


Figure 6. Brick elasticity modulus anisotropy E_x for $E_0 = 12036$ MPa.

Table 4. Theoretical mortar elasticity modulus at $B_{(1)} = 3 - k^2$ ($E_0 = 2140$ MPa).

θ°	0°	15°	30°	45°	60°	75°	90°
$k^2 = 0.5$	4280	3591	2634	2140	2014	2080	2140

Table 5. Theoretical mortar elasticity modulus at $B_{(2)} = \frac{1+5k^2}{3}$ ($E_0 = 2140$ MPa).

θ°	0°	15°	30°	45°	60°	75°	90°
$k^2 = 0.5$	4280	4174	3804	3210	2634	2263	2140

Mortar elasticity modulus anisotropy is shown in Fig. 7.

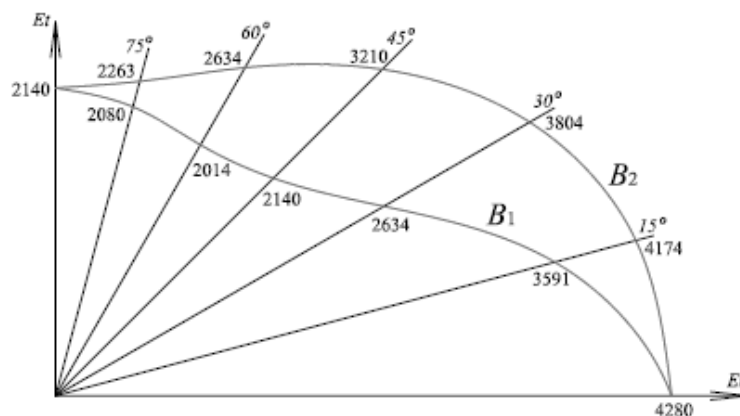


Figure 7. Mortar elasticity modulus anisotropy for $E_0 = 2140$ MPa.

3. Brickwork elasticity modulus in the tangential direction (connection in series):

$$E_t = \frac{E_0^{brick} \cdot E_0^{mortar}}{E_0^{brick} + E_0^{mortar}} = \frac{12036 \cdot 2140}{12036 + 2140} = 1816 \text{ MPa.}$$

Brickwork elasticity modulus in the radial direction (connection in parallel):

$$E_r = E_0^{brick} + E_0^{mortar} = 12036 + 2140 = 14176 \text{ MPa.}$$

Then anisotropic index $k = \sqrt{\frac{E_t}{E_r}} = 0.358$.

The anisotropic index and elasticity parameters calculated by dependencies (see formulas 7, 8) Glukhikh V.N. but with regard for brick and mortar characteristics according to [28, 29] are presented in Table 6.

Table 6. Brickwork anisotropic index and elasticity parameters.

$k^2 = \frac{E_t}{E_r}$	Elasticity Parameters	
	$B_{(1)} = 3 - k^2$	$B_{(2)} = \frac{1 + 5k^2}{3}$
0.128	2.872	0.547

The diagram of anisotropy index – elasticity parameters dependency obtained in work [30] for determining relationships between brickwork elasticity characteristics is shown in Fig. 8.

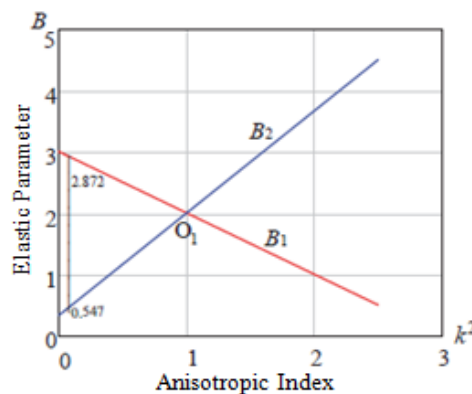


Figure 8. Anisotropy index – brickwork elasticity parameters dependences according to formulas from reference literature.

Therefore, if the barrel vault brick and mortar type are known and with regard for the known formulas (3, 4) according to [28, 29], the brickwork elasticity parameters being the subject of this study are in the field (or within the limit) between the two straight lines (Fig. 8).

The values of theoretical brickwork elasticity moduli are presented in Tables 7, 8.

Table 7. Theoretical brickwork elasticity modulus at $B_{(1)} = 3 - k^2$ ($E_0 = 12036 \text{ MPa}$).

θ°	0°	15°	30°	45°	60°	75°	90°
According to formulas (12, 13) $k^2 = 0.128$	14176	6146	2698	1816	1638	1729	1816

Table 8. Theoretical brickwork elasticity modulus at $B_{(2)} = \frac{1 + 5k^2}{3}$ (MPa).

θ°	0°	15°	30°	45°	60°	75°	90°
According to formulas (12, 13) $k^2 = 0.128$	14176	12092	7660	4337	2698	2006	1816

Brickwork elasticity modulus anisotropy in view of known formulas (10–15) according to [28, 29] is shown in Fig. 9.

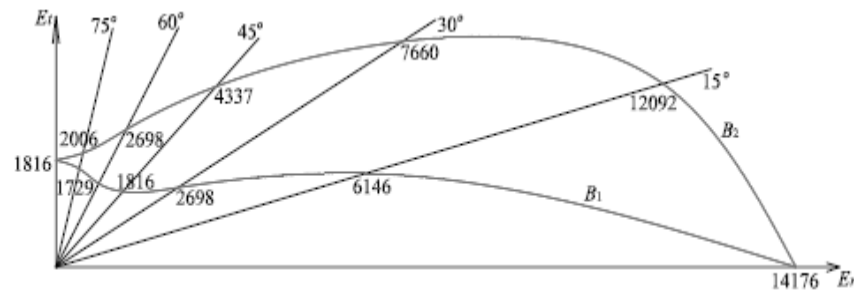


Figure 9. Brickwork elasticity modulus anisotropy (calculated by formulas (3, 4) [31, 32]).

4. Calculation of elasticity constants in a new system of coordinates in view of anisotropy properties in the first group of the elasticity parameter $B_{(1)} = 3 - k^2$, $\theta = 90^\circ$:

$$E_{x'} = \frac{E_r \cdot E_t}{E_t \cdot \cos^4 \theta + E_r \cdot (3 - k^2) \cdot \cos^2 \theta \sin^2 \theta + E_r \cdot \sin^4 \theta} = 1816 \text{ MPa};$$

$$E_{y'} = \frac{E_r \cdot E_t}{E_t \cdot \sin^4 \theta + E_r \cdot (3 - k^2) \cdot \cos^2 \theta \sin^2 \theta + E_r \cdot \cos^4 \theta} = 14176 \text{ MPa};$$

$$G_{rt} = \frac{E_t \cdot G_{rt}}{3 - k^2 + 2 \cdot \mu_{rt}} = 572.528 \text{ MPa},$$

where $\mu_{rt} = 0.15$ is Poisson ratio [32].

$$G_{x'y'} = \frac{E_t \cdot G_{rt}}{G_{rt} \cdot 8 \cdot (k^2 - 1) \cdot \sin^2 \theta \cdot \cos^2 \theta + E_t} = 572.528 \text{ MPa};$$

$$\mu_{x'y'} = -E_{x'} \left[\frac{2(k^2 - 1)}{E_r} \cdot \sin^2 \theta \cdot \cos^2 \theta + \frac{\mu_{rt}}{E_t} \right] = 0.15.$$

Calculation of elasticity constants in a new system of coordinates in view of anisotropy properties in the second group of the elasticity parameter $B_{(2)} = \frac{1 + 5k^2}{3}$, $\theta = 90^\circ$:

$$E_{x'} = \frac{3 \cdot E_r \cdot E_t}{3 \cdot E_t \cdot \cos^4 \theta + E_r \cdot (1 + 5 \cdot k^2) \cdot \cos^2 \theta \sin^2 \theta + 3 \cdot E_r \cdot \sin^4 \theta} = 1816 \text{ MPa};$$

$$E_{y'} = \frac{3 \cdot E_r \cdot E_t}{3 \cdot E_t \cdot \sin^4 \theta + E_r \cdot (1 + 5 \cdot k^2) \cdot \cos^2 \theta \sin^2 \theta + 3 \cdot E_r \cdot \cos^4 \theta} = 14176 \text{ MPa};$$

$$G_{rt} = \frac{E_t \cdot G_{rt}}{1 + 5 \cdot k^2 + 6 \cdot \mu_{rt}} = 2144.44 \text{ MPa};$$

$$G_{x'y'} = \frac{3 \cdot E_t \cdot G_{rt} \cdot 8 \cdot (1 - k^2)}{G_{rt} \cdot 8 \cdot (1 - k^2) \cdot \sin^2 \theta \cdot \cos^2 \theta + 3 \cdot E_t} = 2144.44 \text{ MPa};$$

$$\mu_{x'y'} = -E_{x'} \left[\frac{2 \cdot (1 - k^2)}{3 \cdot E_r} \cdot \sin^2 \theta \cdot \cos^2 \theta - \frac{\mu_{rt}}{E_t} \right] = 0.15.$$

The results are shown in Fig. 10–12 (Option $B_{(1)} = 3 - k^2$ and concentrated loads in $F_{1,2} = 5$ kN).

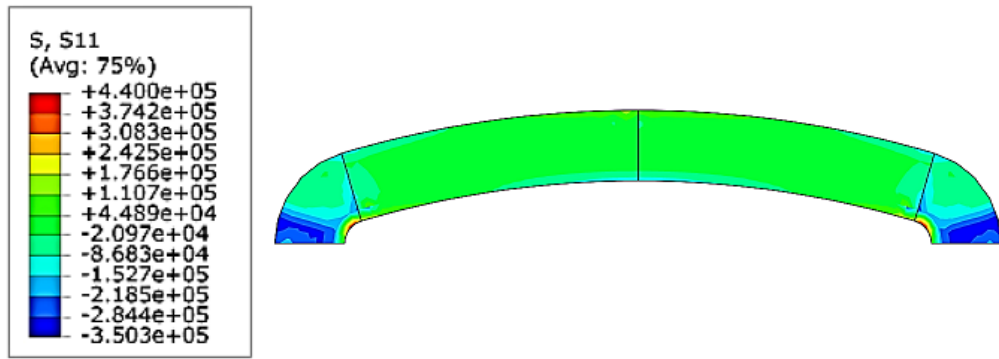


Figure 10. Stress isofields σ_r , Pa.

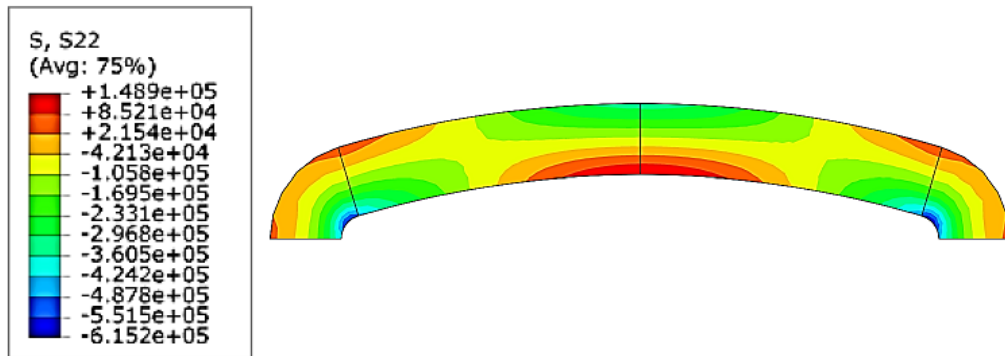


Figure 11. Stress isofields σ_θ , Pa.

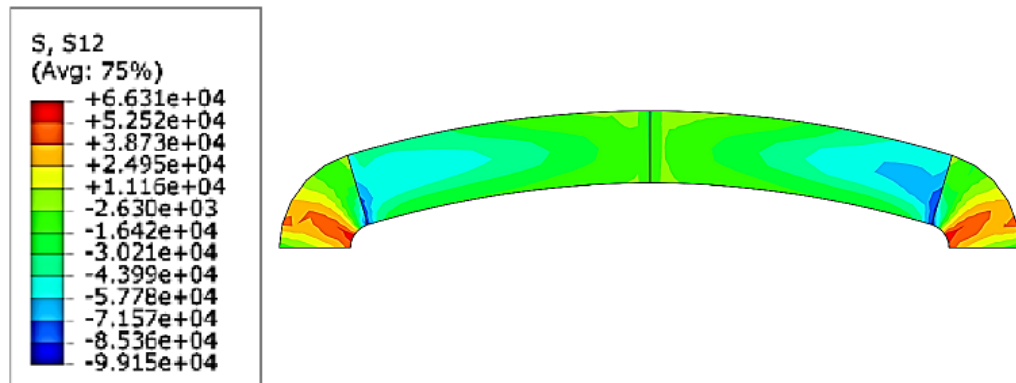


Figure 12. Stress isofields $\tau_{r\theta}$, Pa.

Graphics from the Abacus SW for $B_{(2)} = \frac{1+5k^2}{3}$, $F_{1,2} = 5$ kN (Fig. 13÷15):

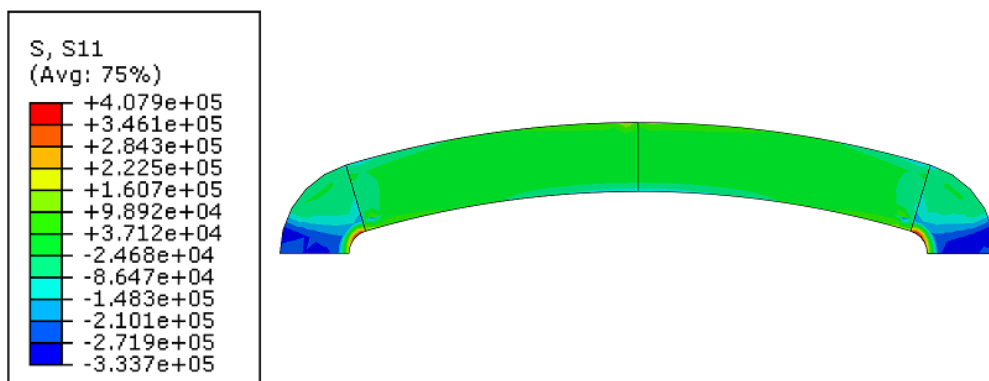


Figure 13. Stress isofields σ_r , Pa.

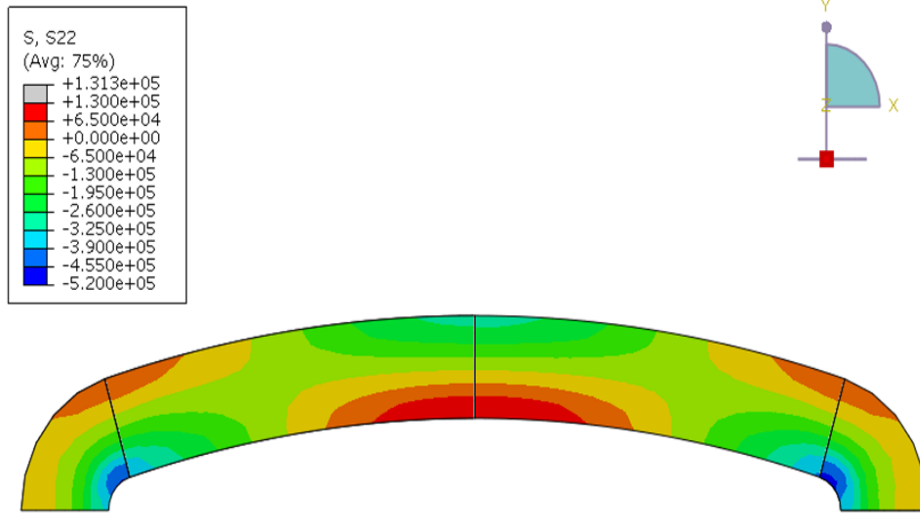


Figure 14. Stress isofields σ_θ , Pa.

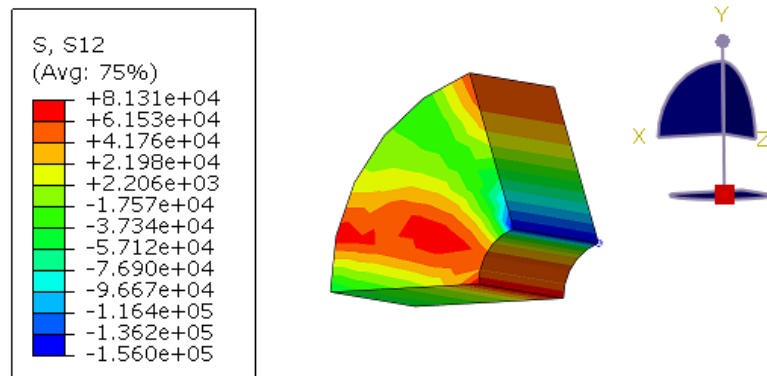


Figure 15. Stress isofields $\tau_{r\theta}$, Pa.

The resulting stress values calculated by two elasticity parameters at the vault head and near the vault abutments are presented in Tables 9–11.

Table 9. Radial stresses σ_r in the vault head ($\varphi = 0^\circ$).

On the external surface, r_d	
$B_{(1)} = 3 - k^2$	$B_{(2)} = \frac{1 + 5k^2}{3}$
σ_r , MPa	σ_r , MPa
-0.045	-0.037

Table 10. Radial stresses σ_r in the vault head ($\varphi = 0^\circ$).

On the internal surface, r_t		On the external surface, r_d	
$B_{(1)} = 3 - k^2$	$B_{(2)} = \frac{1 + 5k^2}{3}$	$B_{(1)} = 3 - k^2$	$B_{(2)} = \frac{1 + 5k^2}{3}$
σ_θ , MPa	σ_θ , MPa	σ_θ , MPa	σ_θ , MPa
0.15	0.13	-0.35	-0.3

Table 11. Tangential σ_θ and shearing $\tau_{r\theta}$ stresses at the intersection of two curves at the abutment.

On the internal surface, r_i		On the middle part, r	
$B_{(1)} = 3 - k^2$	$B_{(2)} = \frac{1 + 5k^2}{3}$	$B_{(1)} = 3 - k^2$	$B_{(2)} = \frac{1 + 5k^2}{3}$
σ_θ , MPa	σ_θ , MPa	$\tau_{r\theta}$, MPa	$\tau_{r\theta}$, MPa
-0.551	-0.475	-0.099	-0.156

Thus, we have performed a numerical analysis of a stress condition using Abaqus 6.14 software package with regard for two elasticity parameters.

Our studies confirm the hypothesis according to which it is required to take into account the properties of materials and the brickwork itself in every specific case in order to improve calculation accuracy.

A well-known work [2] presents curves describing the nature of stress distribution σ_r and σ_θ for an anisotropic circular structure for $k^2 < 1$, $k^2 > 1$, $k^2 = 1$. In the case of materials $E_\theta > E_r$, $k^2 > 1$ stresses decrease as they approach the center, and they become zero at the center. If $E_\theta < E_r$ and $k^2 < 1$, stresses will increase as they approach the center.

It is notable that the relationship between elasticity constants or the so-called anisotropic index (k^2) plays an important role in the analysis of stress strain behavior of orthotropic structures; it is impossible to find out the stress distribution pattern without knowing its numerical value.

According to various sources [28, 29], elasticity constant distribution anisotropic index in cylindrically anisotropic bodies is different. Correspondingly, stress strain behavior will be different in 3 cases under study (bricks, mortar, brickwork). Therefore, a relationship between elasticity constants found out on the basis of experimental strength data in smooth transition from the radial direction to the tangential one is the most suitable one for brickwork.

As it can be seen from the obtained results, the choice of the arch axis outline in the process of survey exercises a significant influence on the obtained arch stress state results.

4. Conclusions

1. This work recommends to take elasticity constant into account for determining the deformation modulus value. We propose a method for determining elasticity constants using elasticity parameters for a barrel vault in the form of a curvilinearly orthotropic anisotropic bar with a cylindrical anisotropy.

2. On the basis of the results of theoretical and experimental studies of well-known Russian scientists, we proposed a diagram connecting elasticity constants for a brickwork barrel vault on the principal anisotropy directions.

3. On the ground of studies performed earlier, we have refined the method of determining elasticity constants on arbitrary directions for a complex brickwork structure as an anisotropic material (bricks and mortar joints).

4. Comparative analysis of the obtained results has proved that the formulas for determining elasticity constants for cylindrically orthotropic anisotropic body can also be used for complex brickwork structures, like flat-arched vaults.

References

- Kaldar-ool, A-Kh.B., Babanov, V.V., Allahverdov, B.M., Saaya, S.S. Additional load on barrel vaults of architectural monuments. Magazine of Civil Engineering. 2018. 08(84). Pp. 15–28. DOI: 10.18720/MCE.84.2
- Lekhnitskiy, S.G. Anisotropic plates. Moscow, 1957. 463 p. (rus)
- Stefanou, I., Sab, K., Heck, J.V. Three dimensional homogenization of masonry structures with building blocks of finite strength: a closed form strength domain. International Journal of Solids and Structures. 2015. No. 54. Pp. 258–270.
- Carini, A., Genna, F. Stability and strength of old masonry vaults under compressive longitudinal loads: Engineering analyses of a case study. Engineering Structures. 2012. No. 40. Pp. 218–229.
- Skripchenko, I.V., Bespalov, V.V., Lukichev, S.Y., Zimin, S.S. Unconventional cases of the stone vaults. Construction of Unique Buildings and Structures. 2017. 2(53). Pp. 87–95.
- Basilio, I., Fedele, R., Lourenco, P.B., Milani, G. Assessment of curved FRP-reinforced masonry prisms: Experiments and modelling. Construction and Building Materials. 2014. No. 51. Pp. 492–505.

7. Milani, G. Upper bound sequential linear programming mesh adaptation scheme for collapse analysis of masonry vaults. *Advances in Engineering Software*. 2015. No. 79. Pp. 91–110.
8. Milani, G., Tralli, A. A simple meso-macro model based on SQP for the non-linear analysis of masonry double curvature structures. *International Journal of Solids and Structures*. 2012. No. 49. Pp. 808–834.
9. Kamal, O.A., Hamdy, G.A., El-Salakawy, T.S. Nonlinear analysis of historic and contemporary vaulted masonry assemblages. *HBRC Journal*. 2014. 10(3). Pp. 235–246.
10. Lalin, V.V., Dmitriev, A.N., Diakov, S.F. Nonlinear deformation and stability of geometrically exact elastic arches. *Magazine of Civil Engineering*. 2019. 5(89). Pp. 39–51. DOI: 10.18720/MCE.89.4
11. Orlovich, R.B., Nowak, R., Vatin, N.I., Bespalov, V.V. Natural oscillations of a rectangular plates with two adjacent edges clamped. *Magazine of Civil Engineering*. 2018. 82(6). Pp. 95–102. DOI: 10.18720/MCE.82.9
12. Rizzi, E., Rusconia, F., Cocchetti, G. Analytical and numerical DDA analysis on the collapse mode of circular masonry arches. *Engineering Structures*. 2014. No. 60. Pp. 241–257.
13. Thavalingam, A., Bicanic, N., Robinson, J.I., Ponniah, D.A. Computational framework for discontinuous modelling of masonry arch bridges. *Composite & Structures*. 2001. No. 79. Pp. 1821–1830.
14. Pottman, H., Eigensatz, M., Vaxman, A., Wallner, J. Architectural geometry. *Computers & Graphics*. 2015. No. 47. Pp. 145–164.
15. Cancelliere, I., Imbimbo, M., Sacco, E. Experimental tests and numerical modeling of reinforced masonry arches. *Engineering Structures*. 2010. No. 32. Pp. 776–792.
16. Ramaglia, G., Lignola, G.P., Prota, A. Collapse analysis of slender masonry barrel vaults. *Engineering Structures*. 2016. Vol. 117. Pp. 86–100.
17. Castori, G., Borri, A., Corradi, M. Behavior of thin masonry arches repaired using composite materials. *Composites Part B: Engineering*. 2016. Vol. 87. Pp. 311–321.
18. De Santis, S., Tomor, A.K. Laboratory and field studies on the use of acoustic emission for masonry bridges. *NDT & E International*. 2013. No. 55. Pp. 64–74.
19. Aydin, A.C., Özkaya, S.G. The finite element analysis of collapse loads of single-spanned historic masonry arch bridges (Ordu, Sarpdere Bridge). *Engineering Failure Analysis*. 2018. Vol. 84. Pp. 131–138.
20. Felice, G. Assessment of the load carrying capacity of multi span masonry arch bridges using fibre beam elements. *Engineering Structures*. 2009. No. 31. Pp. 1634–1647.
21. Madani, K. A study of fiber deboning in circular composite arches. *Comptes Rendus Mecanique*. 2002. No. 330. Pp. 535–541.
22. Zhang, Y., Macorini L., Izzuddin B.A. Mesoscale partitioned analysis of brick-masonry arches. *Engineering Structures*. 2016. Vol. 124. Pp. 142–166.
23. Diaferio, M., Venerito, M., Vitti, M. Experimental Testing and Numerical Analysis of a Barrel Vault. *Engineering Structures*. 2018. Vol. 15. Pp. 138–151.
24. Zimin, S.S., Bespalov, V.V., Kazimirova, A.S. The computational model stone arch. System requirements: Adobe Acrobat Reader. URL: [http://donnasa.ru/publish_house/journals/vestnik/2015/vestnik_2015-3\(113\).pdf](http://donnasa.ru/publish_house/journals/vestnik/2015/vestnik_2015-3(113).pdf). (accessed: August 01, 2018). (rus)
25. Zimin, S.S., Kokotkova, O.D., Bespalov, V.V. Vault structures of historical buildings. *Construction of Unique Buildings and Structures*. 2015. 2(29). Pp. 57–72. (rus)
26. Russian Set of Rules SP 15.13330.2012. Masonry and reinforced masonry structures. The actual formulation of Construction Norms and Regulations II-22-81*. Moscow: FAU "FCS", 2012. 86 p. (rus)
27. Sidorov, V.N. The finite element method in the calculation of structures: theory, algorithm, examples of calculations in the SIMULIA Abaqus software package. Moscow, 2015. 288 p. (rus)
28. Umanskiy, A.A. Guidance book for designers of industrial, residential and public buildings. Calculation and theoretical reference book. 2nd ed., revsed. Moscow, 1972. 599 p. (rus)
29. Residential Building Design Guide. №3. The design of residential buildings (to SNiP 2.08.01-85) 2.08.01-85). Moscow, 1989. 305 p. (rus)
30. Rjanisyn, A.R. Some problems of the mechanics of systems that deform in time. M-St. Petersburg, 1949. 252 p. (rus)
31. Ugolev, B.N. Deformability and stresses in wood during drying. Moscow, 1971. 174 p. (rus)
32. Yakovlev, K.P. Brief physico-technical reference book. Moscow, 1960. 412 p. (rus)

Contacts:

Anay-Khaak Kaldar-ool, oorzhaka-h@mail.ru

Vladimir Glukhikh, tehme@spbgasu.ru

Eres Opubl, fduecnufce@mail.ru

Svetlana Saaya, sedip@list.ru